The experimental charge-density approach in the evaluation of intermolecular interactions. Application of a new module of the *XD* programming package to several solids including a pentapeptide

Yu. A. Abramov,* A. Volkov, G. Wu and P. Coppens

Department of Chemistry, State University of New York at Buffalo, Buffalo, New York 1460-3000, USA. Correspondence e-mail: chem9989@acsu.buffalo.edu

A new module interfaced to the *XD* programming package has been used in the evaluation of intermolecular interactions and lattice energies of the crystals of *p*-nitroaniline, L-asparagine monohydrate and the pentapeptide Boc-Gln–D-Iva–Hyp–Ala–Phol (Boc = butoxycarbonyl, Iva = isovaline = ethylalanine, Phol = phenylalaninol). The electrostatic interactions are evaluated with the atom-centered distributed multipoles from KRMM (κ'-restricted multipole model) refinements, using the Buckingham expression for non-overlapping charge densities. Results for *p*-nitroaniline are compared with Hartree–Fock (HF), density functional (DFT) and Møller-Plesset (MP2) supermolecular calculations and with HF and DFT periodic calculations. The HF and DFT methods fail to predict the stability of the *p*-nitroaniline crystal but the results of the experimental charge-density approach (ECDA) are in good agreement with both MP2 interaction energies and the experimental lattice energy. ECDA results for L-asparagine monohydrate compare well with those from DFT supermolecular and periodic HF calculations. The disorder of the terminal group in the pentapeptide, which persists at the experimental temperature of 20 K, corresponds to an energy difference of only 0.35 kJ mol^{-1}, which is too small to be reproduced with current methods.

1. Introduction

The recent development of area detectors has opened new horizons for the use of X-ray diffraction in charge-density analysis. The importance of the charge density is evident from the Hohenberg–Kohn (1964) theorem, according to which all ground-state properties are unique functionals of the charge density. An intrinsic feature of the X-ray charge density is that it reflects all many-body effects, which are often not available from *ab initio* calculations. This makes it an attractive tool for the study of a broad spectrum of problems of physical and chemical interest. Much insight into chemical bonding can be gained by evaluation of the topological properties of the charge density as defined by the AIM (atoms in molecules) theory (Bader, 1990), and of its electrostatic properties, including the energy, the potential, and the atomic and molecular moments (Coppens, 1997). Methods for the topological analysis of experimental charge densities have been described in a number of recent publications (Souhassou & Blessing, 1999; Flensburg & Madsen, 2000; Volkov *et al.*, 2000).

The experimental charge-density approach (ECDA) to intermolecular interactions was pioneered by Spackman (Spackman, 1986*b*; Spackman *et al.*, 1988). In this approach, the anisotropic electrostatic interaction energy derived from atom-centered multipoles ($E_{\text{es}}^{\text{mul}}$) is combined with the van der Waals interaction energy (U_{vdW}) evaluated with isotropic atom–atom exp−6 potentials:

$$E_{\text{int}} = E_{\text{es}}^{\text{mul}} + U_{\text{vdW}} \qquad (1)$$

$$U_{\text{vdW}} = \sum_{ij} A_{ij} \exp(-B^* R_{ij}) - C/R_{ij}^6. \qquad (2)$$

The first exp −6 term of the atom–atom potentials (2) approximates the short-range exchange-repulsion energy between monomer charge distributions, while the second term represent the dispersion energy. The atom–atom potentials of Spackman (1986*a*) were derived theoretically from the electron-gas model within the Kim & Gordon (1974) approximation, and combined with dispersion-energy parameters. The exchange-repulsion term was omitted for polar H atoms participating in strong hydrogen bonding.

In our version of the ECDA method (Abramov, Volkov, Wu & Coppens, 2000; Abramov, Volkov & Coppens, 2000), a perturbation-theory-based atom–atom potential of the polar

hydrogen of Mitchell & Price (1989) was introduced, and the crucial effect of the basis-set overlap error in the multipole refinement was reduced by use of the κ'-restricted model (KRMM). In the KRMM method, exponents of the atomic deformation functions are fixed at average values derived by multipole refinement of theoretical structure factors (Abramov *et al.*, 1999). The basis-set overlap error originates in the lack of physical constraints, such as the Pauli exclusion principle, in the multipole refinement of overlapping molecular charge densities. The calculations presented here use the Mitchell & Price potential for polar hydrogen as optimized by Coombes *et al.* (1996).

To eliminate correlation between quadrupole populations and thermal parameters for H atoms, we have proposed constraining the ratio of the dipole and quadrupole populations of H atoms in strong hydrogen bonds as a linear function of the hydrogen-to-acceptor distance. The linear dependence used is based on refinement of theoretical static structure factors (Abramov, Volkov & Coppens, 2000).

Contrary to the other force-field methods based on theoretical charge densities of isolated molecules, dimers or trimers (Stone, 1996; Price, 1996; Beachy *et al.*, 1997; Stern *et al.*, 1999), the multipole expansion of the electrostatic energy within ECDA in principle includes the contributions of polarization, charge transfer and electron correlation effects. However, in the approach the increase in the molecular internal energy on polarization is neglected. As was pointed out recently by Suponitsky *et al.* (1999), this increase equals 50% of the gain in the intermolecular interaction energy due to the polarization, assuming a linear response to the external field and its derivatives. A more consistent and more general treatment, based on the distributed polarizability description of polarizable molecules, was given earlier by Stone (1996).

However, the satisfactory agreement between ECDA results and *ab initio* calculations (Abramov, Volkov & Coppens, 2000; Abramov, Volkov, Wu & Coppens, 2000) indicates that this error does not have a large effect, even for highly polarizable systems. It is possible that the polarization energy is partially canceled by the underestimate of the penetration energy.

In the case of the non-centrosymmetric crystal of urea, de Vries *et al.* (2000) argued that, because of phase uncertainties, the electrostatic contribution to the intermolecular interaction energy, E_{es}^{mul}, as evaluated from the X-ray experiment, may be biased, although it has been demonstrated that the multipole model is able to retrieve accurate structure-factor phases, at least for error-free theoretical data (Spackman & Byrom, 1996).

In the present study, a new program, *XDINTER*, is used to apply the ECDA method to crystals of *p*-nitroaniline (PNA), L-asparagine·H_2O and the pentapeptide Boc–Gln–D-Iva–Hyp–Ala–Phol (PP). As in our previous studies (Coppens *et al.*, 1999; Abramov, Volkov, Wu & Coppens, 2000; Abramov, Volkov & Coppens, 2000), the ECDA results are compared with the supermolecular and *ab initio* periodic crystal calculations. Whenever possible, lattice energies are compared with sublimation enthalpy values.

2. Methods

The program *XDINTER* uses the Ewald lattice summation for the terms up to dipole–dipole interactions (Smith, 1998) in the evaluation of the binding energy of an infinite crystal. As higher-order contributions decrease faster with distance, they may be evaluated by summation of the pairwise interactions over an increasing number of neighboring unit cells. In addition, the program can be used to evaluate the molecular binding energy of a central molecule with conformational changes. The effect of small shifts from the molecular equilibrium position can also be calculated.

The electrostatic intermolecular interaction energy is obtained *via* the atom-centered multipole expansion in the Cartesian tensor formulation (Buckingham, 1978; Coppens, 1997):

$$E_{es}^{mul}(AB) = Tq_Aq_B + T_\alpha(q_A\mu_{\alpha,B} - q_B\mu_{\alpha,A}) + T_{\alpha\beta}(\tfrac{1}{3}q_A\Theta_{\alpha\beta,B}$$
$$+ \tfrac{1}{3}q_B\Theta_{\alpha\beta,A} - \mu_{\alpha,A}\mu_{\beta,B}) + \ldots . \qquad (3)$$

Here, q, μ_α and $\Theta_{\alpha\beta}$ are charge, dipole and quadrupole atomic electrostatic moments, $T_{\alpha\beta\ldots\nu} = (4\pi\varepsilon_0)^{-1}\nabla_\alpha\nabla_\beta\ldots\nabla_\nu R_{AB}^{-1}$ is a Cartesian tensor, the indices α, β, γ, ... denote x, y or z and Einstein summation over repeated indices is implied. As the refinements used here included only terms with $l \leq 3$, the expansion (3) was truncated at the octupole–octupole ($\sim R^{-7}$) term. The direct relationship between atom-centered multipoles from the aspherical atom refinement of the X-ray data and the atomic electrostatic moments (Coppens, 1997) is used in the calculation. The pairwise atom–atom potentials may be the most uncertain part of the ECDA method. In *XDINTER*, alternative sets of atom–atom parameters may be supplied by the user. The Spackman (1986a) potentials used in the current study were parameterized non-empirically and are appropriate for calculations based on the charge-density distribution of a periodic system. In contrast, the Williams & Cox (Cox *et al.*, 1981; Williams & Cox, 1984) potentials, which are also incorporated in the program, are parameterized empirically and, thus, effectively absorb attractive contributions such as polarization, charge transfer and electrostatic penetration. Thus, these potentials could be recommended for calculations based on the procrystal charge densities constructed from non-interacting molecules. The default choice of the atom–atom potential for polar H atoms participating in strong hydrogen bonds is that of Coombes *et al.* (1996). In the current study, the presence of hydrogen bonds was verified by topological analysis of the charge density (Bader, 1990). Further details on the program are given in Appendix A.

3. Theoretical calculations

The periodic Hartree–Fock (PHF) and density functional (PDFT) calculations of the PNA crystal with the *CRYSTAL95* software package (Dovesi *et al.*, 1996) have been described previously (Abramov, Volkov & Coppens, 2000). *CRYSTAL98* (Saunders *et al.*, 1999) PHF calculations on the L-asparagine·H_2O crystal were performed at the PHF/6-31G**

Table 1
Intermolecular interaction energies in the PNA dimers (kJ mol^{-1}).

Dimer‡	HF/6-311G**	B3LYP/6-311G**	MP2/6-31G**	ECDA† Experimental	ECDA† PHF/6-31G**
A	−11.5	−14.1	−14.8	−32.7 (53)	−29.5
B	−19.9	−23.8	−23.4	−41.4 (80)	−46.0
C	−15.4	−14.6	−17.6	−26.9 (54)	−36.4
D	+5.0	+1.1	−28.0	−19.8 (13)	−29.9
E	+4.0	−0.6	−18.1	−30.6 (70)	−20.5

† The experimental charge-density approach was based either on experimental structure factors or on structure factors generated from the PHF/6-31G** calculations. For the former, e.s.d.s, based on monopole errors only, are given in parentheses. ‡ The crystallographic geometries of dimers are presented in Fig. 2.

Table 2
Binding energies (kJ mol^{-1}).

Crystal	ECDA†	PHF/6-21G**	PHF/6-31G**	PDFT/6-21G**‡
p-Nitroaniline	−106.7 (115)	−10.8	−10.1	+2.0
L-Asparagine·H₂O	−242.4 (167)	–	−266.5	–

† From experiment. E.s.d.'s in parentheses. ‡ PDFT calculations with Becke (1988) exchange and Perdew & Wang (1992) correlation functionals (BPWGGA).

level of theory. The shrinking factor of the Monkhorst net (Monkhorst & Pack, 1976) was set equal to 10, giving 216 **k** points in the reciprocal space of this crystal. The Gillat shrinking factor (Gillat, 1972) was set to 18, and 10 plane waves were used for the expansion of the eigenvalues e_k. The basis set was modified for the hydrogen and carbon atoms as described previously (Abramov, Volkov, Wu & Coppens, 2000; Abramov, Volkov & Coppens, 2000).

The binding energy of L-asparagine monohydrate was calculated with the *CRYSTAL98* program as the difference between the energy of the molecular hydrate in the crystal and the energy of the isolated dimeric unit in the crystal geometry. The theoretical basis-set superposition error, which occurs when the energy of a supermolecule or crystal is compared with that of its components (Kestner & Combariza, 1999), was corrected by adopting the counterpoise method (Boys & Bernardi, 1970). For the crystal calculations, ghost atoms were located at atomic positions within 3.15 Å from the atoms in the original molecule. The molecular relaxation energies upon sublimation were evaluated with the *Gaussian94* program package (Frisch *et al.*, 1995) at the MP2/6-31G** level of theory.
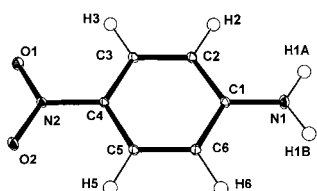
Figure 1
Molecular structure of *p*-nitroaniline.

The supermolecular calculations of the dimer interaction energies were performed with the *Gaussian94* and *NWCHEM3.3.1* (Bernholdt *et al.*, 1995) program packages, using the experimental molecular geometry.

4. Results

4.1. *p*-Nitroaniline

20 K synchrotron data on PNA (Fig. 1), collected at the SUNY X3 beamline at NSLS (Wu & Coppens, 1999), were used in this study. The data were refined with the KRMM model (Abramov *et al.*, 1999). Several types of relatively strong intermolecular interactions can be distinguished in the crystal (Fig. 2): a network of C—H···O and N—H···O hydrogen bonds (Figs. 2a–c), the antiparallel-displaced stacking interaction (Fig. 2d) and a pseudo-stacking interaction between two canted molecules (Fig. 2e). The corresponding ECDA intermolecular interaction energies based on both the experimental and the theoretical (PHF/6-31G**) structure factors are compared with the supermolecular dimer calculations at the HF, B3LYP and MP2 levels of theory in Table 1. For the hydrogen-bonded dimers, the overall agreement between supermolecular calculations is satisfactory at all levels (Table 1, Figs. 2a–c). Owing to the inclusion of many-body interactions in the crystal, the ECDA energies are higher than the corresponding supermolecular results. However, for the other two stacking-type dimers (Figs. 2d, e), HF and DFT, but not MP2, calculations fail to describe the considerable stabilizing interaction between the monomers. This is not surprising as the dispersion rather than the electrostatic term gives the dominant contribution to the stacking interaction energy (Fig. 2d). For the interaction between the two canted molecules, the two terms are of comparable size (Fig. 2e). The dispersion-energy term is not accounted for at the HF and DFT levels of theory (see *e.g.* Hobza & Sponer, 1999).

The PNA binding energies in the crystal according to the ECDA, PHF/6-21G**, PHF/6-31G** and PDFT/6-31G** calculations are compared in Table 2. The failure of the PHF and PDFT to describe the dispersion energy manifests itself in the very small values of the corresponding binding energies. In contrast to the electrostatic interactions, the intermediate-range dispersion interactions, which are strong in aromatic systems, are always attractive. Accordingly, in spite of the strong hydrogen bonding, the dominant contribution to the PNA binding energy is the dispersion term, the electrostatic, exchange-repulsion and dispersion contributions being −91.8,

Table 3
Lattice energies (kJ mol^{-1}).

Crystal	ECDA†	PHF/6-21G**	PHF/6-31G**	PDFT/6-21G**
p-Nitroaniline	−96.5 (115)	−0.6	+0.1	+12.2
L-Asparagine·H$_2$O	−98.7 (167)	–	−122.8	–

† From experiment. E.s.d.'s in parentheses.

Table 4
Intermolecular interaction energies in the dimers displaying hydrogen bonding in the L-asparagine·H$_2$O crystal (kJ mol^{-1}).

Symmetry operation	Hydrogen bond	$R_{\text{H}\cdots\text{O}}$ (Å)	B3LYP/6-311G**	ECDA† Experimental	PHF/6-31G**
−1/2 − X, −Y, Z + 1/2	N—H(5)···O(3)	1.77	−36.8	−36.2 (135)	−81.4
X − 1/2, 1/2 − Y, −Z	N—H(4)···O(2)	1.82	−40.0	−49.8 (190)	−42.4
1 − X, Y − 1/2, 1/2 − Z	N—H(2)···O(1)	1.85	−40.4	−40.6 (38)	−41.7
1.5 − X, Y, Z − 1/2	O—H(1)···O(1)	1.86	−20.8	−19.3 (17)	−12.9
1/2 − X, −Y, Z − 1/2	N—H(6)···O(1)	1.90	−45.4	−49.4 (214)	−108.1
X, Y, Z	N—H(3)···O(4)	1.92	−24.0	−7.2 (24)	−31.7
1 − X, 1/2 + Y, 1/2 − Z	N—H(7)···O(2)	2.11	−69.1	−71.8 (98)	−158.6
2 − X, Y − 1/2, 1/2 − Z	C—H(8)···O(4)	2.37	−7.9	−7.9 (14)	−25.7

† The experimental charge-density approach was based either on experimental structure factors or on structure factors generated from the PHF/6-31G** calculations. For the former, e.s.d.'s are given in parentheses.

99.3 and −114.1 kJ mol^{-1}, respectively, according to the ECDA calculations. Similar observations concerning the crucial importance of the dispersion term have been reported recently for crystals of 2-amino-5-nitropyridine and 2-amino-5-nitro-1,3-pyrimidine (Stone & Tsuzuki, 1997), p-benzoquinone (Cardenas-Jiron *et al.*, 2000) and p-amino-p'-nitrobiphenyl (Abramov, Volkov & Coppens, 2000).

The PNA molecular relaxation energy as evaluated at the MP2/6-31G** level of theory is equal to −10.2 kJ mol^{-1}. In order to evaluate the PNA lattice energy, this value was subtracted from the results for the binding energy. While the PHF and PDFT calculations do not predict the crystals to be stable, a reasonable result of −96.5 (114) kJ mol^{-1} is obtained using ECDA (Table 3). It agrees well with the experimental sublimation enthalpy of 98–109 kJ mol^{-1} (Chickos, 1987).

4.2. L-Asparagine monohydrate

The X-ray charge-density analysis of the strongly hydrogen-bonded L-asparagine·H$_2$O crystal was reported recently (Arnold *et al.*, 2000). The molecular geometry is shown in Fig. 3(*a*). The intermolecular interaction energies, based on the earlier multipole refinement results, agree very well with the supermolecular B3LYP/6-311G** results (Table 4). The agreement implies that the anticipated enhancement of the intermolecular interactions due to induced polarization of the long and polar L-asparagine molecules is not observed.

When the ECDA is applied with the theoretical HF structure factors, the resulting interaction energies are generally much larger than the experimental values (Table 4). To some extent, this may be expected, as the electrostatic inter-

molecular interaction energies are enhanced in the HF method owing to the neglect of electron correlation (Abramov, Volkov, Wu & Coppens, 2000). However, scaling of the PHF electrostatic terms by the appropriate factor of 0.76 (Abramov, Volkov, Wu & Coppens, 2000) is not sufficient to remove the larger discrepancies.

The ECDA calculation of the asparagine·H$_2$O binding energy agrees within two standard deviations with the PHF result (Table 2). In order to evaluate the lattice energy, the relaxation energy of the asparagine·H$_2$O complex, which reflects the dissociation of the dimer and the geometry relaxation of the isolated asparagine and water molecules, was subtracted from the corresponding binding energy. It is equal to −143.7 kJ mol^{-1} according to the MP2/6-31G** calculations. The optimized geometry of the isolated asparagine molecule corresponds to the neutral form with a strong N—H···O intramolecular hydrogen bond not found in the crystal (Fig. 3*b*). The resulting lattice energies are presented in Table 3. No experimental sublimation enthalpy is available for L-asparagine monohydrate.

4.3. Boc-Gln–D-Iva–Hyp–Ala–Phol

The structure of the pentapeptide Boc-Gln–D-Iva–Hyp–Ala–Phol (PP) was first analyzed by Ciszak *et al.* (1999). With the exception of the protein crambin (Jelsch *et al.*, 2000), this compound is, with 97 atoms, among the largest analyzed so far by detailed X-ray charge-density methods, the pentapeptide studied by Lecomte, Benard and co-workers (Wiest *et al.*, 1994) being of similar size. It is the first molecule of this size to be analyzed with He-temperature synchrotron data. The data on PP (space group $P2_12_12_1$) were collected at 20 K using 0.664 Å radiation from a synchrotron source (217226 reflections measured, 17144 unique reflections). The full analyses including topological evaluation of the atomic properties will be described in a separate communication (Wu *et al.*, 2001). The molecular structure is presented in Fig. 4. The molecule in the crystal has two conformations, the atoms of the terminal H$_2$COH group of the phenylalaninol unit being disordered (Fig. 4), with 89 and 11% occupations of the *A* and *B* configurations at 20 K, respectively. At room temperature, the two orientations have equal occupancy (Ciszak *et al.*, 1999).

In the multipole refinement, all non-hydrogen atoms were refined anisotropically, subject to a rigid-bond constraint. The

final R factor (2.2%) attests to the quality of the data. Full details on the charge density and its topological analysis will be reported elsewhere.

The ECDA binding energies of the PP molecule in the pure crystals of the A and B conformers are calculated as −500 (32) and −413 (31) kJ mol^{-1}, respectively. However, a parallel PDFT calculation with a 3-21G** basis set gives a binding energy for the crystal of A that is smaller by a factor of about two (Wu *et al.* 2001). This discrepancy, which requires further analysis, must be related to a large difference in polarity of the molecule, as expressed by its dipole moment, which is ~30 D according to the experiment (configuration A), but only 14 D according to the calculation.

To simulate the energetics of the structural disorder, the effect of replacing one molecule A by B at the center of a cluster of A molecules, 27 and 125 unit cells large, was evaluated. The resulting changes of the total intermolecular interaction energies in the clusters are calculated as 40 (6) and 42 (6) kJ mol^{-1}, respectively. As these energies depend only slightly on the size of the cluster, they are predominantly determined by the nearest-neighbor interactions. The energy difference, which is in accordance with the preference for the A configuration in the crystal, is in part compensated by the intramolecular energy difference of two conformers, which favors B because of its intramolecular O–H$\cdots$O hydrogen bond. We have performed *ab initio* HF calculations on the molecule in the geometry of each of the conformers. Using 4-31G** and 6-311G** basis sets, energy differences of, respectively, 9.58 and 10.04 kJ mol^{-1} are obtained. These values are differences between very large total electronic energies of the conformers and should be used with caution.

The Boltzmann distribution, $n_A/n_B = \exp(-\Delta E/RT)$, predicts a total energy difference of only 0.35 kJ mol^{-1} for the given occupations of the conformers A and B in the crystal at 20 K. This difference is too small to be reproduced with current methods, either experimental or theoretical. At more elevated temperatures, the entropy contribution becomes dominant, leading to the observed 1:1 distribution at room temperature.

5. Conclusions

The agreement of the ECDA results with the theoretical and calorimetric values is generally satisfactory, except for the pentapeptide, which is the largest molecule studied so far by the methods employed here. The effect of phase uncertainties and of the approximations used in the analysis will be the subject of further studies. Alternative choices of atom–atom parameters will be considered in future studies when accurate data on more crystals are available for ECDA analysis.

APPENDIX A
The program *XDINTER*

The program *XDINTER* utilizes the experimental charge-density approach to the intermolecular interaction-energy

calculations. *XDINTER* is based on the Hansen–Coppens multipole model (Coppens, 1997) and requires XD.RES and XD.MAS files of the *XD* program package (Koritsanszky *et al.*, 1997) as input files. An XD.COV file is also needed for the e.s.d. calculations. An additional unformatted module must be included in the XD.MAS file in order to define the parameters and tasks for the calculations:

```
!!!!!!!!!!!!!!!!!!!!!!!!!!!!!!!!!!!!!!!
MODULE *XDINTER
!
!select the options for the calculations
SELECT  *laten ewald esd  *neutr *spack wilcox param
!
!set parameters of the Ewald summation
EWALD   kmax 10 alpha 0.5 uccut 2 rcut 100.0
!
!generate the symmetry-related molecule for intermolecular interactions
!APPLY  symm 1 translations  0.  0.  0. only   ato(1) ato(2) ...
!APPLY  symm 1 translations  0.  0.  0. except ato(1) ato(2) ...
!
!define the polar hydrogens
!HPOLAR  ato(1) ato(2) ...
!
!skip atoms in the original molecule
!SKIP    ato(1) ato(2) ...
!
!modify the original molecule
!MODIFY MOVE 0.0 0.0 0.0
!MODIFY SKIP ato(1) ato(2) ...
!
END  XDINTER
!!!!!!!!!!!!!!!!!!!!!!!!!!!!!!!!!!!!!!!
```

The standard parameters of the deformation-density radial functions (exponent and powers of distance) from the *XD* program package are incorporated for first- and second-row atoms. The atomic monopole populations can be rescaled (*neutr*) to produce a neutral molecule if necessary (Spackman, 1992). The standard deviations of the interaction and lattice energies can be evaluated (*e.s.d.*) using variance/covariance elements for the monopole population parameters from the corresponding XD.COV file.

Currently, two sets of exp−6 atom–atom potentials are incorporated in the program: Spackman's (1986a) (*spack*) and Williams & Cox's (Cox *et al.*, 1981; Williams & Cox, 1984) (*wilcox*). Both sets are complemented by the atom–atom potential for polar hydrogen atoms (*HPOLAR*) participating in strong hydrogen bonds as optimized by Coombes *et al.* (1996) (A_{HpHp} = 5029.6 kJ mol^{-1}, C_{HpHp} = 21.5 kJ Å^6 mol^{-1}, B_{HpHp} = 4.66 Å^{-1}).

The following options are available in the program.

The intermolecular interaction energies between the original molecule or its fragment and the symmetry-generated molecule or its fragment can be calculated.

The binding energy (*laten*) can be calculated by applying the Ewald summation up to the dipole–dipole term (Smith, 1998). In the case of an acentric unit cell, the use of the Ewald summation scheme is crucial to achieve reasonable convergence. All other contributions may be evaluated by summation of the pairwise interactions over an increasing number of neighboring unit cells (up to ±*uucut* cells along each crystallographic axis) until convergence. For the estimation of the lattice energy (ignoring zero-point energy), the molecular relaxation energy upon sublimation must be subtracted from the binding energy.

The interaction energy of a modified molecule with a cluster of surrounding unmodified molecules can be evaluated. The modification of the original molecule can be performed by
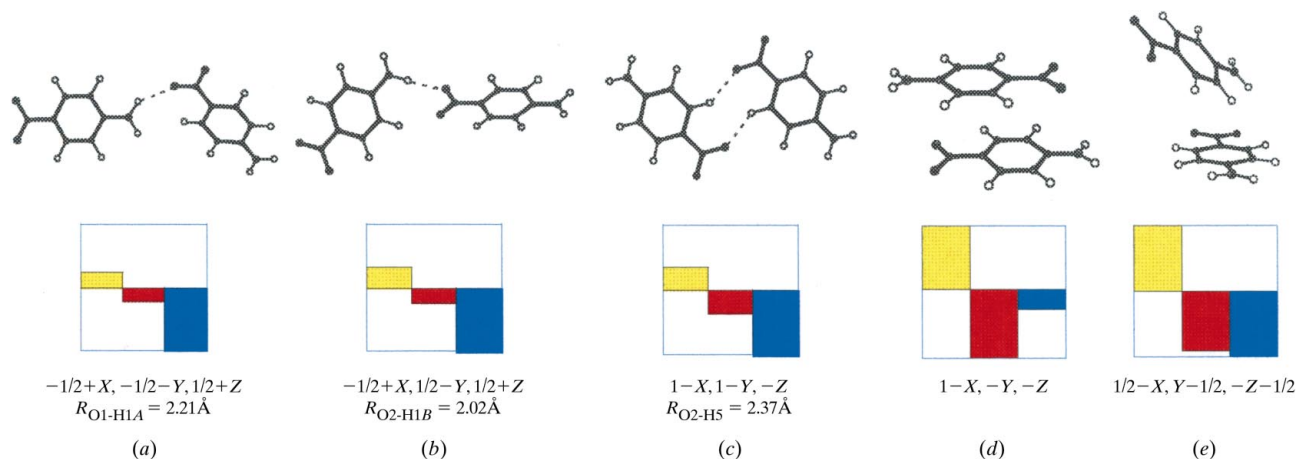
Figure 2
Geometry of molecular pairs displaying the strongest interactions in the PNA crystal. Relative contributions of the exchange-repulsion (yellow column), dispersion (red column) and electrostatic (blue column) terms to the intermolecular interaction energies in the dimers are illustrated below.
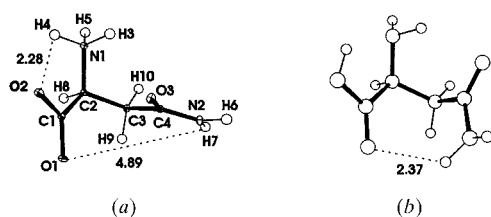

Figure 3
(a) Crystallographic and (b) MP2/6-31G** optimized molecular structures of asparagine. Intramolecular hydrogen bonding occurs only in the optimized structure. Distances in Å.

shifting its coordinates relative to the equilibrium position (*MODIFY MOVE*) or/and by changing its conformation or substitution (*MODIFY SKIP*). The latter option is useful, for example, for the evaluation of the interaction energy of one conformation of a disordered molecule with a cluster of molecules with another conformation.
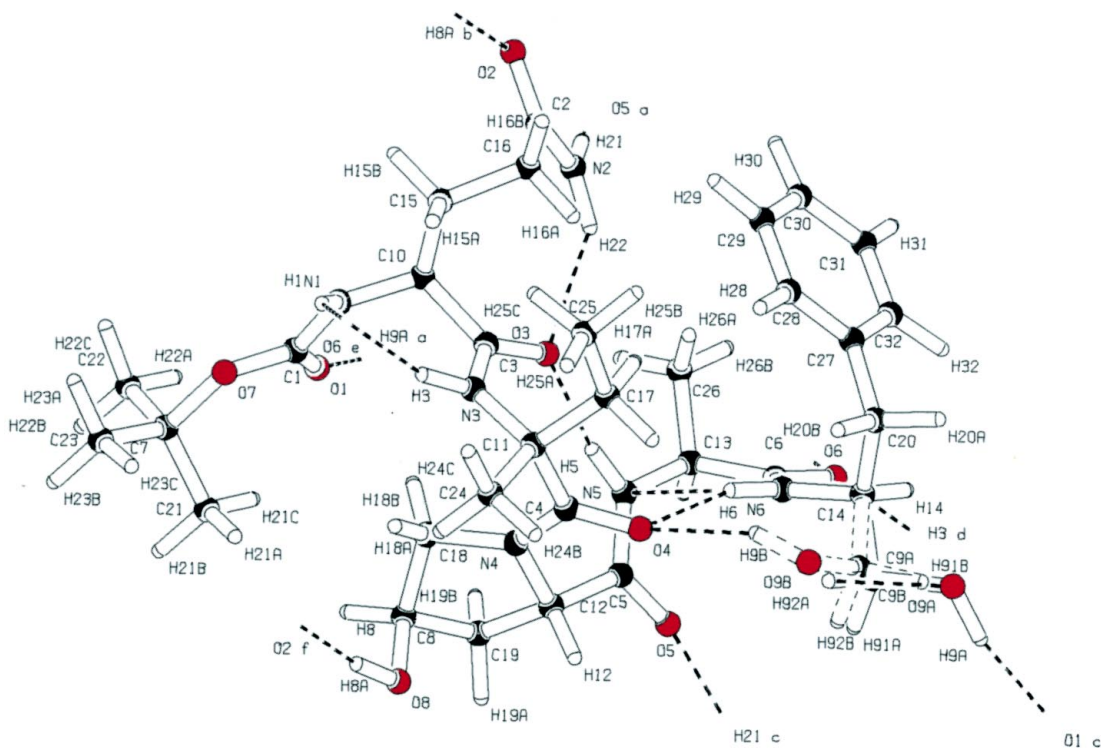
Figure 4
Molecular structure of the pentapeptide Boc-Gln–D-Iva–Hyp–Ala–Phol. The disorder of the CH_2OH group is visible at the lower right of the figure.

References

Abramov, Yu. A., Volkov, A. V. & Coppens, P. (1999). *Chem. Phys. Lett.* **311**, 81–86.

Abramov, Yu. A., Volkov, A. V. & Coppens, P. (2000). *J. Mol. Struct. (Theochem.).* In the press.

Abramov, Yu. A., Volkov, A. V., Wu, G., Coppens, P. (2000). *J. Phys. Chem. B*, **104**, 2183–2188.

Arnold, W. D., Sanders, L. K., McMahon, M. T., Volkov, A. V., Wu, G., Coppens, P., Wilson, S., Godbout, N. & Oldfield, E. (2000). *J. Am. Chem. Soc.* **122**, 4708–4717.

Bader, R. F. W. (1990). *Atoms in Molecules – a Quantum Theory.* Oxford: Clarendon Press.

Beachy, M. D., Chasman, D., Murphy, R. B., Halgren, T. A. & Friesner, R. A. (1997). *J. Am. Chem. Soc.* **119**, 5908–5920.

Becke, A. D. (1988). *Phys. Rev. A*, **38**, 3098–3100.

Bernholdt, D. E., Apra, E., Fruchtl, H. A., Guest, M. F., Harrison, R. J., Kendall, R. A., Kutteh, R. A., Long, X., Nicholas, J. B., Nichols, J. A., Taylor, H. L., Wong, A. T., Fann, G. I., Littlefield, R. J. & Nieplocha, J. (1995). *Int. J. Quantum Chem. Symp.* **29**, 475–483.

Boys, S. F. & Bernardi, F. (1970). *Mol. Phys.* **19**, 553–566.

Buckingham, A. D. (1978). *Intermolecular Interactions: from Diatomics to Biopolymers*, edited by B. Pullman, pp. 1–67. New York: Wiley.

Cardenas-Jiron, G. I., Masunov, A. & Dannenberg, J. J. (2000). *J. Phys. Chem. A*, **103**, 7042–7046.

Chickos, J. S. (1987). *Molecular Structure and Energetics, Physical Measurements*, edited by J. F. Liebman & A. Greenberg, Vol. 2, pp. 6–50. New York: VCH Publishers.

Ciszak, E., Miller R. & Smith, G. D. (1999). Private communication.

Coombes, D. S., Price, S. L., Willock, D. J. & Leslie, M. (1996). *J. Phys. Chem.* **100**, 7352–7360.

Coppens, P. (1997). *X-ray Charge Densities and Chemical Bonding.* New York: Oxford University Press.

Coppens, P., Abramov, Yu. A., Carducci, M., Korjov, B., Novozhilova, I., Alhambra, C. & Pressprich, C. (1999). *J. Am. Chem. Soc.* **121**, 2585–2593.

Cox, S. R., Hsu, L. Y. & Williams, D. E. (1981). *Acta Cryst.* A**37**, 293–301.

Dovesi, R., Saunders, V. R., Roetti, C., Causà, M., Harrison, N. M., Orlando, R. & Aprà, E. (1996). *CRYSTAL95 User's Manual.* University of Torino, Torino, Italy.

Flensburg, C. & Madsen, D. (2000). *Acta Cryst.* A**56**, 24–28.

Frisch, M. J., Trucks, G. W., Schlegel, H. B., Gill, P. M., Johnson, B. G., Robb, M. A., Cheeseman, J. R., Keith, T., Petersson, G. A., Montgomery, J. A., Raghavachari, K., Al-Laham, M. A., Zakrzewski, V. G., Ortiz, J. V., Foresman, J. B., Cioslowski, J., Stefanov, B. B., Nanayakkara, A., Challacombe, M., Peng, C. Y., Ayala, P. Y., Chen, W., Wong, M. W., Andres, J. L., Replogle, E. S., Gomperts, R., Martin, R. L., Fox, D. J., Binkley, J. S., Defrees, D. J., Baker, J., Stewart, J. P., Head-Gordon, M., Gonzalez, C. & Pople, J. A. (1995). *Gaussian94, Revision E.2.* Pittsburgh, PA: Gaussian Inc.

Gillat, G. J. (1972). *J. Comput. Phys.* **10**, 432–465.

Hobza, P. & Sponer, J. (1999). *Chem. Rev.* **99**, 3247–3276.

Hohenberg, P. & Kohn, W. (1964). *Phys. Rev. B*, **136**, 864–871.

Jelsch, C., Teeter, M. M., Lamzin, V., Pichon-Pesme, V., Blessing, R. H. & Lecomte, C. (2000). *Proc. Natl Acad. Sci. USA*, **97**, 3171–3176.

Kestner, N. R. & Combariza, J. E. (1999). *Reviews in Computational Chemistry*, edited by K. B. Lipkowitz & D. B. Boyd, Vol. 13, pp. 99–132. New York: Wiley.

Kim, Y. S. & Gordon, R. G. (1974) *J. Chem. Phys.* **66**, 1842–1850.

Koritsanszky, T., Howard, S., Richter, T., Su, Z., Mallinson, P. R. & Hansen, N. K. (1997). *XD – a Computer Program Package for Multipole Refinement and Analysis of Electron Densities from Diffraction Data.* Free University of Berlin, Berlin, Germany.

Mitchell, J. B. O. & Price, S. L. (1989). *Chem. Phys. Lett.* **154**, 267–272.

Monkhorst, H. J. & Pack, J. D. (1976). *Phys Rev. B*, **13**, 5188–5192.

Perdew, J. P. & Wang, Y. (1992). *Phys. Rev. B*, **45**, 13244–13249.

Price, S. L. (1996). *J. Chem. Soc. Faraday Trans.* **92**, 2997–3008.

Saunders, V. R., Dovesi, R., Roetti, C., Causà, M., Harrison, N. M., Orlando, R. & Zicovich-Wilson, C. M. (1999). *CRYSTAL98 User's Manual.* University of Torino, Torino, Italy.

Smith, W. (1998). *CCP5 Newsletter*, **46**, 18–30.

Souhassou, M. & Blessing, R. H. (1999). *J. Appl. Cryst.* **32**, 210–217.

Spackman, M. A. (1986a). *J. Chem. Phys.* **85**, 6579–6586.

Spackman, M. A. (1986b). *J. Chem. Phys.* **85**, 6587–6601.

Spackman, M. A. (1992). *Chem. Rev.* **92**, 1769–1797.

Spackman, M. A. & Byrom, P. G. (1996). *Acta Cryst.* B**52**, 1023–1035.

Spackman, M. A., Weber, H. P. & Craven, B. M. (1988). *J. Am. Chem. Soc.* **110**, 775–782.

Stern, H. A., Kaminski, G. A., Banks, J. L., Zhou, R., Berne, B. J. & Friesner, R. A. (1999). *J. Phys. Chem. B*, **103**, 4730–4737.

Stone, A. J. (1996). *The Theory of Intermolecular Forces. International Series of Monographs on Chemistry*, Vol. 32. New York: Oxford University Press.

Stone, A. J. & Tsuzuki, S. (1997). *J. Phys. Chem. B*, **101**, 10178–10183.

Suponitsky, K. Yu., Tsirelson, V. G. & Feil, D. (1999). *Acta Cryst.* A**55**, 821–827.

Volkov, A., Gatti, C., Abramov, Yu. A. & Coppens, P. (2000). *Acta Cryst.* A**56**, 252–258.

Vries, R. Y. de, Feil, D. & Tsirelson, V. G. (2000). *Acta Cryst.* B**56**, 118–123.

Wiest, R., Pichon-Pesme, V., Benard, M. & Lecomte, C. (1994). *J. Phys. Chem.* **98**, 1351–1362.

Williams, D. E. & Cox, S. R. (1984). *Acta Cryst.* B**40**, 404–417.

Wu, G., Abramov, Yu. A., Volkov, A. & Coppens, P. (2001). In preparation.

Wu, G. & Coppens, P. (1999). Unpublished results.